# Flexomagnetic effect in frustrated triangular magnetic structures

Pavel Lukashev*
*Department of Physics and Astronomy, University of Nebraska–Lincoln, Lincoln, Nebraska 68588-0299, USA*

Renat F. Sabirianov*
*Department of Physics, University of Nebraska at Omaha, Omaha, Nebraska 68182, USA*
(Received 30 March 2010; published 10 September 2010)

We report appearance of the net magnetization in Mn-based antiperovskite compounds as a result of the external strain gradient (*flexomagnetic effect*). In particular, we describe the mechanism of the magnetization induction in the $Mn_3GaN$ at the atomic level in terms of the behavior of the local magnetic moments of the Mn atoms. We show that the flexomagnetic effect is linear and results from the nonuniformity of the strain, i.e., it is absent not only in the ground state but also when the applied external strain is uniform. We estimate the flexomagnetic coefficient to be $\sim 2\ \mu_B$ Å. We show that at the moderate values of the strain gradient ($\sim 0.1\%$) the flexomagnetic contribution to the net induced magnetization is comparable with the nonlinear contribution. Finally, we apply a classical Heisenberg model to study the correlation between spin-exchange interaction and flexomagnetism, using time quantified Monte Carlo simulation. This confirms the linear nature of the flexomagnetic effect and helps understanding phenomenological aspects behind it.

DOI: 10.1103/PhysRevB.82.094417 PACS number(s): 75.50.−y, 75.80.+q

## I. INTRODUCTION

Magnetomechanical coupling in crystals has many practical applications, such as in sensors, magnetic recording devices, etc. The correlation between external strain and induced magnetization is, in principal, significant for the systems with different dimensionality, i.e., bulk, thin film, and nanoconfigurations. Yet, the correlation between the strain gradient and induced magnetization is especially important in nanostructures and thin-film heterostructures because of the large surface-to-volume ratio which may result in a large surface tension due to the structural distortions caused by lattice mismatch, external stress, etc. For example, the strain gradient may play a significant role when thin film is epitaxially grown on a substrate with slightly different lattice parameters. On the other hand, in problems concerning bulk structures the strain gradient is small and has only negligible contribution. This is so because of the dimensional scaling inherent in the very definition of the strain gradient, i.e., the decrease in the characteristic length of the system, $x$ results in increase in the $\Delta x/x$ ratio. Figure 1 schematically shows possible geometries of the systems under external strain gradient: bent nanowire and nanopill grown on a substrate. The "in-plane" and "out-of-plane" orientations of the induced magnetization shown in Fig. 1 will be explained later in the text.

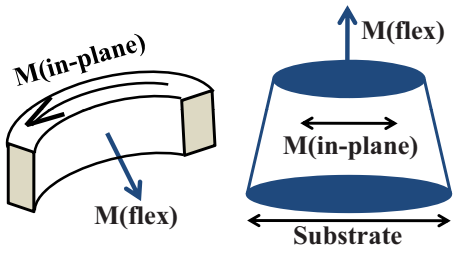


FIG. 1. (Color online) Schematic picture of the systems under strain gradient with possible orientations of the induced magnetization.

The magnetomechanical coupling is phenomenologically described by adding additional terms to the expression for the thermodynamic potential, i.e., free energy, proportional to the product of the magnetic field component and the conjugate terms involving mechanical strain

$$F_{magn} = -\lambda_{i,jk} H_i \sigma_{jk} - \mu_{i,jk} H_i \sigma_{jk}^2 - \nu_{ijkl} H_i \frac{\partial \sigma_{jk}}{\partial x_l}; \qquad (1)$$

$$i,j,k,l = 1,2,3,$$

where $\lambda_{i,jk}$ is the piezomagnetic tensor, $H_i$ is the $i$th component of the magnetic field ($i=x,y,z$), $\sigma_{jk}$ is the elastic stress tensor, $\mu_{i,jk}$ is the magnetoelastic tensor, $\nu_{ijkl}$ is the four-rank tensor (*flexomagnetic tensor*), and $\frac{\partial \sigma_{jk}}{\partial x_l}$ is the strain gradient. For example, piezomagnetic (magnetostrictive) properties of certain antiferromagnetic (AFM) materials are reflected in a term linear both in the magnetic field and in the elastic stress tensor.[1] For the bulk structures the last term on the rhs of Eq. (1) is usually omitted because of its negligible contribution, yet in nanostructures and/or thin-film heterostructures it may play a significant role.

By taking partial derivative of Eq. (1) wrt magnetic field component, $H_i$ we get the net magnetization in the system, which may be linear wrt the strain (piezomagnetic effect), quadratic (second-order magnetoelastic effect), and proportional to the strain gradient

$$M_i = \underbrace{\lambda_{i,jk}\sigma_{jk}}_{piezo} + \underbrace{\mu_{i,jk}\sigma_{jk}^2}_{mag\text{-}elast} + \underbrace{\nu_{ijkl}\frac{\partial \sigma_{jk}}{\partial x_l}}_{flex}; \quad i,j,k,l = 1,2,3. \qquad (2)$$

It is important to emphasize that the symmetries of the $\lambda_{i,jk}$ and $\mu_{i,jk}$ tensors are different from the symmetry of the $\nu_{ijkl}$ tensor in Eq. (2), which means that the induced magnetization will have three contributions, in principal, distinguishable by symmetry arguments only. Moreover, it is possible that because of the crystal and magnetic symmetry the

 

linear piezomagnetism will be absent in the system with the nonzero strain-gradient-induced magnetization. We define the contribution to the $M_i$ from the third term on the rhs of Eq. (2) as *flexomagnetic* (FlM) *effect*, i.e., strain-gradient-induced magnetization.

To the best of our knowledge the term *flexomagnetoelectric effect* was first coined by Bobylev and Pikin in their study of the correlation between elastic and electromagnetic properties of nematic liquid crystals.[2] As a sidenote we emphasize here that in their work Bobylev and Pikin discussed the "reverse" flexomagnetoelectricity, i.e., the reorientation (which they called *flex*) of the molecules under external electric and magnetic fields. Much work was done in the past to investigate the correlation between electric polarization and external strain gradient, at both experimental and theoretical levels.[3–7] Yet, the correlation between magnetic behavior of the system and the gradient of the strain was not the subject of mainstream research. To the best of our knowledge there is only one recent publication on this subject,[8] which presents theoretical study of the spontaneous flexoelectric/flexomagnetic effect in nanoferroics. One of the reasons for the insufficient study on this matter is the obvious complexity of the problem—as opposed to the flexoelectric effect, where the electric polarization directly correlates with the atomic displacements, the FlM effect is indirect, i.e., it results from the reorientation of the atomic spins following the atomic displacements (because of the spin-exchange interactions). As a result, for the FlM effect one has to consider not only the crystal but also the magnetic structure and symmetry. Systems of interest must satisfy certain conditions, such as they have to be nonmagnetic in ground state, and at the same time they have to exhibit strong magnetoelastic coupling. Comparatively well-known manifestation of these properties is the piezomagnetic effect, i.e., induction of a spontaneous magnetic moment in the system under mechanical strain. In what follows we present the results of our study of the external strain-gradient-induced magnetization mechanism.

## II. Mn-BASED ANTIPEROVSKITES

To understand the mechanism of flexomagnetism at the atomic level we perform first-principles study for the $Mn_3GaN$ under strain gradient. The choice of the material is based on the intriguing magnetomechanical coupling mechanism in $Mn_3GaN$. In its ground state $Mn_3GaN$ is antiferromagnetic with noncollinear $\Gamma^{5g}$ structure (in the classification of Bertaut *et al.*[9]), i.e., the Mn local magnetic moments (LMMs) on the (111) plane form clockwise or counterclockwise configuration, such that the spin moments in the plane are compensating each other. The atoms of Mn, Ga, and N form an antiperovskite (AP) crystal structure, and the lattice constant of the primitive five-atom cell of $Mn_3GaN$ is 3.86 Å. Figure 2 shows the unit cell of the $Mn_3GaN$ in the ground state.

In our recent work[10] we have shown that the application of the external stress to the Mn-based AP compounds results in appearance of the nonzero magnetic moment, i.e., these compounds exhibit *piezomagnetic* properties. This can be explained from the symmetry viewpoint, i.e., as a result of the applied biaxial strain the symmetry of the system reduces from the trigonal space group $P\bar{3}1m$ to the orthorhombic $Pm'm'm$ ferromagnetic space group. Because of this transition some of the symmetry operations are not compatible anymore with the new structure. The appearance of the net magnetization in the system under external stress is due to the rotation of the LMMs of the Mn atoms from their equilibrium positions. After rotation the LMMs in the (111) plane become inequivalent and do not compensate each other anymore. The piezomagnetic effect is linear and magnetization reversal is potentially possible upon reversal of the sign of the strain (compressive to tensile or vice versa). In the present work we examine the magnetic behavior of the $Mn_3GaN$ under strain gradient (*flexure*), i.e., we look at the third term on the rhs of Eq. (2).

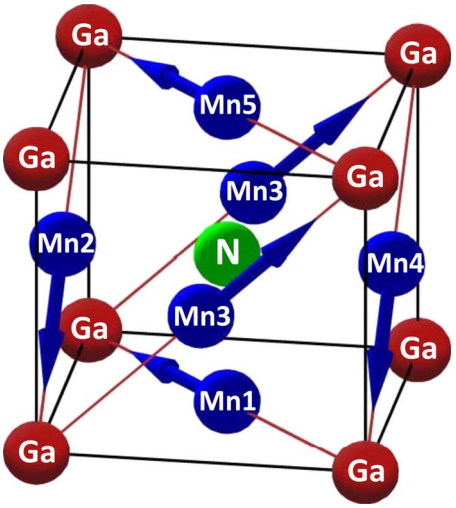


FIG. 2. (Color online) Ground state of the antiperovskite $Mn_3GaN$ unit cell: noncollinear $\Gamma^{5g}$ magnetic structure. Local magnetic moments are shown by blue arrow on Mn atoms.

## III. COMPUTATIONAL METHOD

We use projector augmented wave (PAW) method by Blöchl,[11] implementation of PAW by Kresse and Joubert[12] in the Vienna *ab initio* simulation package (VASP) code within a Perdew-Burke-Ernzerhof generalized gradient approximation[13] of the density-functional theory. We use a $3\times12\times6$ $k$-point sampling for the supercell of 40 atoms and the Blöchl's tetrahedron integration method.[14] We set the plane-wave cut-off energy to 300 eV and we choose the convergence criteria for energy of $10^{-5}$ eV.

## IV. MODEL AND RESULTS

Accurate electronic-structure calculations require periodic boundary condition. The strain gradient breaks the periodicity of the primitive unit cell, therefore to construct a model with translational symmetry we have to take larger cell. For $Mn_3GaN$ the smallest possible configuration to retain the translational symmetry under external strain gradient consists of the eight primitive cells of $Mn_3GaN$ ($4\times2\times1$ cell

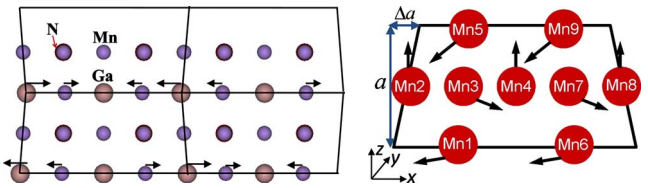


FIG. 3. (Color online) Left panel: $Mn_{24}Ga_8N_8$ cell: four-domain structure. Mn atoms—blue, Ga atoms—gray, and N atoms—dark red (almost invisible behind Mn atoms). The directions of the atomic shifts are schematically shown by black arrows. Right panel: single domain in $Mn_{24}Ga_8N_8$ under strain gradient. The arrangement of local magnetic moments of Mn is shown with the easy axis along the (010) direction.

configuration). To simulate the strain gradient we introduce small relative atomic shifts of Ga and Mn atoms in a way, which splits our 40-atom cell in four domains (see Fig. 3, left panel). In each of the four domains we have strain gradient, $\Delta a/a$ (schematically shown on the right panel of the Fig. 3) and four-domain configuration satisfies the periodic boundary condition. The initial orientation of the LMMs forms noncollinear $\Gamma^{5g}$ structure. Due to the spin-orbit coupling there is an anisotropy in the system causing the magnetic moments of Mn atoms into (111) plane as was shown experimentally (Fig. 2). If spin-orbit coupling is not included (its magnitude is very small) the easy axis is arbitrary. For convenience, in Fig. 3 (right panel) we show the arrangement of local magnetic moments of Mn with the easy axis along the viewing direction, i.e., along (010) direction. Table I summarizes the values for the atomic shifts and the strain gradients for the $Mn_{24}Ga_8N_8$ cell.

Next we relax the LMMs of the Mn atoms but we keep the atomic positions fixed to make sure that the crystal structure does not relax back to the unstrained ground state. Figure 4 shows results of our calculations for the magnetization per Mn atom as a function of the strain gradient. There are two different contributions: the blue line with circles represents out-of-plane magnetization (multiplied by 10) which is a direct result of the flex. If the strain applied to the cell is uniform then from the symmetry arguments it is clear that only in-plane magnetization will appear. The black line with squares represents in-plane nonlinear contribution to the magnetization which results from the in-plane rotations of the LMMs of the Mn atoms. Important feature of these two mechanisms is that at the moderate values of the strain gradient the contributions of the linear flexomagnetic and the nonlinear in-plane magnetizations are comparable. Although for calculated values of strain gradient the contribution of the flexomagnetic effect to magnetization is smaller than that of nonlinear magnetoelastic effect, the relative contribution of the flexomagnetic effect is increasing with the decreasing strain gradient due to its linear nature (dependence on strain gradient) while nonlinear magnetoelastic effect is quadratic in its lowest power. The comparable nature of the linear contribution at the moderate gradient values is important for the practical applications where the regular values of the strain gradient are on the order of ~0.1–0.2 %.

TABLE I. Atomic shifts of Mn and Ga atoms and strain gradients (flex): $Mn_{24}Ga_8N_8$.

| Step | Mn (Å) | Ga (Å) | Flex (%) |
|---|---|---|---|
| 1 | 0.01868 | 0.03736 | 0.242 |
| 2 | 0.03736 | 0.07442 | 0.484 |
| 3 | 0.05589 | 0.11179 | 0.724 |
| 4 | 0.07450 | 0.14900 | 0.965 |
| 5 | 0.09264 | 0.18528 | 1.200 |
| 6 | 0.11132 | 0.22234 | 1.442 |

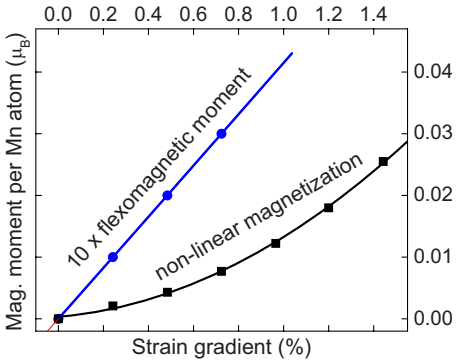


FIG. 4. (Color online) Linear out-of-plane (×10) (blue circles) and nonlinear in-plane (black squares) induced net magnetization of Mn atom as a function of the strain gradient.

To understand better the nature of these two contributions we examine the behavior of in-plane and out-of-plane components of the LMMs of Mn atoms within one domain. Figures 5 and 6 show our results. The out-of-plain contribution comes from the Mn atoms 3, 4, and 7 (see Fig. 3, right panel). The zero components for the out-of-plane magnetization of certain Mn atoms (1, 2, 5, 6, 8, and 9) are due to the symmetry of the model which is made of four domains. These specific atoms are located at the domain boundaries (as shown in Fig. 3, right panel) and cannot have out-of-plane magnetization. We emphasize here that Figs. 5 shows out-of-plane components not the values of local magnetic moments (the latter are nonzero and comparable for all the Mn atoms).

With the chosen direction of the strain gradient along $z$ axis (Fig. 3), the Mn atoms along the $y$ axis in consecutive

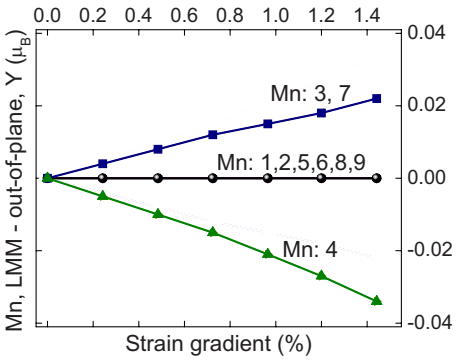


FIG. 5. (Color online) Out-of-plane magnetic moment vs strain gradient.

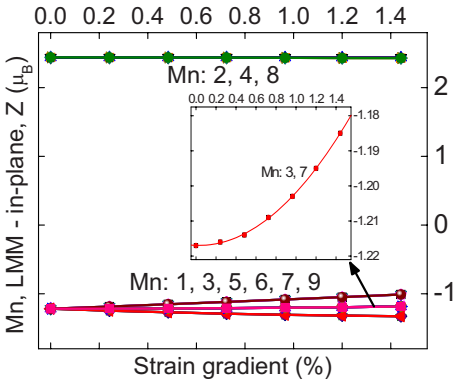


FIG. 6. (Color online) In-plane magnetic moment vs strain gradient.

(111) planes are, in fact, the second Mn-Mn neighbors. Because of this they are arranged ferromagnetically. As a result the magnetization induced along $y$ axis in neighboring planes does not cancel despite AFM coupling between nearest neighbors.

At the same time the in-plane rotations of the Mn LMMs (atoms 3 and 7) show distinct nonlinear feature, which contributes to the nonlinear in-plane magnetization dependence on the applied strain shown in Fig. 4. The appearance of the out-of-plane component of magnetization is not observed if the applied strain is uniform. Therefore, the appearance of the linear out-of-plane magnetization is purely strain-gradient-related effect and its mechanism is different from the one responsible for the in-plane magnetization induction.

## V. FLEXOMAGNETIC COEFFICIENT

We estimate the flexomagnetic coefficient at the strain gradient value of ~0.4% from Eq. (2) and the magnetization vs strain gradient data shown in Fig. 4 as follows:

$$M_{flex} = \nu \frac{\partial \sigma}{\partial x} = \nu \overleftrightarrow{C} \frac{\partial \epsilon}{\partial x},$$

$$\frac{\partial \epsilon}{\partial x} = \frac{\partial}{\partial x}\left[\frac{\Delta a_0}{a_0}\right] = \frac{\partial}{\partial x}\left[\frac{a_0 + c \cdot x}{a_0}\right] = \frac{1}{a_0} c \approx \frac{0.004}{3.9 \times 10^{-10}\ \mathrm{m}},$$

$$\nu \overleftrightarrow{C} = M_{flex} / \frac{\partial \epsilon}{\partial x} = \frac{0.002 \mu_B}{0.004/3.9 \times 10^{-10}\ \mathrm{m}} \Rightarrow \nu C \sim 2 \mu_B \text{Å}.$$

Here we used the following general relation between stress and strain:

$$\sigma_{jk} = C_{jkgh} \epsilon_{gh}; \quad j,k,g,h = 1,2,3, \tag{3}$$

where $C_{jkgh}$ is the elasticity tensor. In our case we estimated only one component of the product $\nu C$, since we consider one-dimensional strain gradient in our model. Besides, here $a_0 = 3.9 \times 10^{-10}$ m is the ground-state lattice constant of the $Mn_3GaN$, $M_{flex} = 0.002 \mu_B$ is the induced out-of-plane magnetization value at ~0.4% of the strain gradient ($c$ is the gradient coefficient). Since the magnetization is linear, the $\nu$ will have the same value over the considered range of the strain gradient.

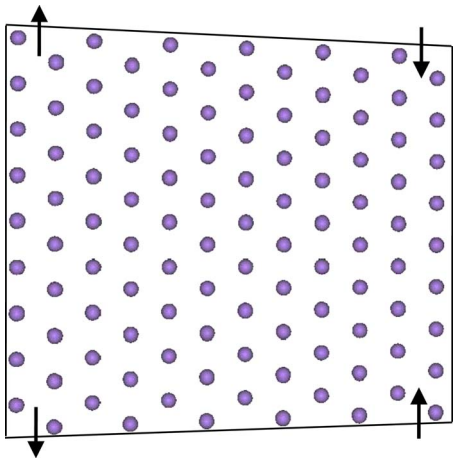

FIG. 7. (Color online) Monte Carlo model of 54 triangular lattices of Mn atoms in 9×6 two-dimensional grid: black arrows represent compression/expansion directions.

## VI. SPIN-EXCHANGE INTERACTION: HEISENBERG MODEL

Qualitatively, the out-of-plane component of the magnetization can be explained by the changes in the exchange interactions under strain gradient. Interatomic distances between nearest neighbors become position dependent (nonuniform) when strain gradient is applied. This is schematically shown on the right panel of the Fig. 3 where, for example, the Mn1 ↔ Mn4 distance becomes larger than the Mn4 ↔ Mn5 distance. This nonuniformity of interatomic distances is not present in the ground state and in the case of the uniform strain. The decrease in the interactomic distance between Mn4 and Mn5 results in the increase in the exchange interaction, represented in the Heisenberg Hamiltonian by the pair-exchange parameter $J(\mathbf{r}_{4,5})$ (see Fig. 3, right panel) due to the increasing overlap of their wave functions, and at the same time increase in the distance between Mn1 and Mn4 results in the decrease in the $J(\mathbf{r}_{1,4})$. This mechanism is responsible for the out-of-plane rotation of the Mn4 (and other "inside of the domain" Mn atoms, such as Mn3 and Mn7 in the Fig. 3, right panel) LMM.

To better understand the correlation between spin exchange and flexomagnetism we apply a classical Heisenberg model in a way, which simulates the effect of the strain gradient on the frustrated triangular lattice at zero temperature. In our particular model we take 54 triangular lattices in 9 ×6 two-dimensional grid (see Fig. 7). The directions of the strain are shown in Fig. 7 by black arrows. We assume interactions between nearest neighbors to be antiferromagnetic and the ground-state calculation confirms the triangular magnetic lattice. The magnetization was calculated in terms of the exchange interaction as follows. The Heisenberg model Hamiltonian is

$$H = \sum_{i>j} J_{ij} \vec{S}_i \vec{S}_i, \tag{4}$$

where $J_{ij} = J_{eq}[1 + (dJ/J_{eq})\epsilon(x)]$ is Heisenberg pair-exchange parameter. $\epsilon = \Delta(r - r_0)/r_0$ is a local strain parameter, show-

ing the partial change in the interatomic distance relative to its unstrained distance. The gradient-strain-related parameter, $dJ/J_{eq}$ is chosen to be negative, i.e., the Heisenberg exchange parameter decreases in magnitude with the increase in the interatomic distance.

The choice of the finite triangular lattice is driven by the symmetry of this lattice which does not allow the piezomagnetic effect, i.e., the application of the uniform strain does not result in the appearance of the magnetization. Thus, the magnetization which appears under applied strain gradient is purely due to the flexomagnetic effect. Furthermore, the arrangement of spins in adjacent (111) plains of $Mn_3GaN$ is antiferromagnetic, i.e., the curls of spin density in adjacent (111) plains are oppositely directed (as schematically shown in the Fig. 2). Therefore, the appearance of the out-of-plane magnetization should occur in each (111) plane in system under strain gradient. Besides, Mn and Ga atoms on the (111) plane of the fcc structure (shown in the Fig. 2) indeed form a triangular lattice. Thus, although the finite triangular lattice model we consider (Fig. 7) does not exactly represent the $Mn_3GaN$, it should provide a key to the qualitative understanding of flexomagnetic effect in frustrated triangular lattices with AFM interactions.

We use the time quantified Monte Carlo (MC) simulation[15] to analyze the magnetization of triangular lattice. We fixed the radius of the conical section to $R=0.1$. We used $2\times10^5$ steps of MC simulations and repeated process till the averaged magnetization would change to $1\times10^{-3}$. Error bars were estimated from the last four runs. While the ground state of the triangular lattice has no net magnetization, we observe the induction of magnetization upon application of strain gradient. The net and the out-of-plane magnetizations are shown in Fig. 8 as a function of flex (in units normalized to a number of spins). Thus, the piezomagnetic tensor has at least two nonzero components. The induced out-of-plane magnetization is much smaller than the in-plane one. The flexomagnetic coefficient is larger in the finite nanostructure considered in our classical model than the one found for the small domain in $Mn_3GaN$. This is due to the suppression of the edge contribution in the first-principles model arising from the symmetry of the model which uses periodic boundary conditions.

Thus, we conclude that the main mechanism behind flexomagnetism is spin-exchange interaction being function of interatomic distances. In particular, when external strain gradient is applied these distances become inequivalent, which results in out-of-plane rotations of local magnetic moments. As a result of these rotations, system acquires nonzero net magnetic moment.

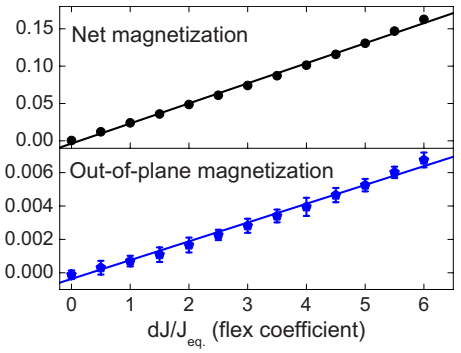


FIG. 8. (Color online) Net (top panel) and out-of-plane (bottom panel) magnetization: Monte Carlo simulation.

## VII. CONCLUSIONS

In summary, in this paper we discussed the appearance of the net magnetization in Mn-based antiperovskite compounds (in particular, $Mn_3GaN$) under external strain gradient (flexomagnetic effect). The magnetization dependence on the *flexure* is linear. The estimated flexomagnetic coefficient is $\sim 2\mu_B$Å. Although for calculated values of strain gradient the contribution of the flexomagnetic effect to magnetization is smaller than that of nonlinear magnetoelastic effect, the relative contribution of the flexomagnetic effect is increasing with the decreasing strain gradient due to its linear nature (dependence on strain gradient), while nonlinear magnetoelastic effect is quadratic in its lowest power of strain. At the strain gradients of 0.1% their extrapolated contributions are of the same order of magnitude. To the best of our knowledge, these results have not been confirmed experimentally yet. We hope that our findings will stimulate further research on this subject.

## ACKNOWLEDGMENTS

This work was supported by the National Science Foundation and the Nanoelectronics Research Initiative through the Materials Research Science and Engineering Center at the University of Nebraska. This work was completed utilizing the Blackforest Cluster Computing Facility of the College of Information Science and Technology at University of Nebraska at Omaha.

*Also at Nebraska Center for Materials and Nanotechnology, University of Nebraska-Lincoln, Lincoln, Nebraska 68588.

[1] L. D. Landau, E. M. Lifshitz, and L. P. Pitaevskii, *Electrodinamika Sploshnykh Sred (Electrodynamics of Continuous Media)* (Fizmatlit, Moscow, 2005).

[2] Yu. P. Bobylev and S. A. Pikin, Pis'ma Zh. Tekh. Fiz. **5**, 1032 (1979) [Sov. Tech. Phys. Lett. **5**(9), 430 (1979)].

[3] A. K. Tagantsev, Zh. Eksp. Teor. Fiz. **88**, 2108 (1985) [Sov. Phys. JETP **61**, 1246 (1985)].

[4] V. L. Indenbom, E. B. Loginov, and M. A. Osipov, Kristallografiya **26**, 1157 (1981) [Sov. Phys. Crystallogr. **26**, 656 (1981)].

[5] W. Ma, Phys. Scr. **T129**, 180 (2007).

[6] P. Zubko, G. Catalan, A. Buckley, P. R. L. Welche, and J. F.

Scott, Phys. Rev. Lett. **99**, 167601 (2007).
[7] J. Hong, G. Catalan, J. F. Scott, and E. Artacho, J. Phys.: Condens. Matter **22**, 112201 (2010).
[8] E. A. Eliseev, A. N. Morozovska, M. D. Glinchuk, and R. Blinc, Phys. Rev. B **79**, 165433 (2009).
[9] E. F. Bertaut, D. Fruchart, J. P. Bouchaud, and R. Fruchart, Solid State Commun. **6**, 251 (1968).
[10] P. Lukashev, R. F. Sabirianov, and K. Belashchenko, Phys. Rev. B **78**, 184414 (2008).
[11] P. E. Blöchl, Phys. Rev. B **50**, 17953 (1994).
[12] G. Kresse and D. Joubert, Phys. Rev. B **59**, 1758 (1999).
[13] J. P. Perdew, K. Burke, and M. Ernzerhof, Phys. Rev. Lett. **77**, 3865 (1996).
[14] P. E. Blöchl, O. Jepsen, and O. K. Andersen, Phys. Rev. B **49**, 16223 (1994).
[15] U. Nowak, R. W. Chantrell, and E. C. Kennedy, Phys. Rev. Lett. **84**, 163 (2000).